



CERN-PH-EP-2011-229

LHCb-PAPER-2011-040

November 1, 2018

First observation of the decays

$$\bar{B}^0 \rightarrow D^+ K^- \pi^+ \pi^- \text{ and}$$

$$B^- \rightarrow D^0 K^- \pi^+ \pi^-$$

The LHCb Collaboration ¹

Abstract

First observations of the Cabibbo suppressed decays $\bar{B}^0 \rightarrow D^+ K^- \pi^+ \pi^-$ and $B^- \rightarrow D^0 K^- \pi^+ \pi^-$ are reported using 35 pb^{-1} of data collected with the LHCb detector. Their branching fractions are measured with respect to the corresponding Cabibbo favored decays, from which we obtain $\mathcal{B}(\bar{B}^0 \rightarrow D^+ K^- \pi^+ \pi^-)/\mathcal{B}(\bar{B}^0 \rightarrow D^+ \pi^- \pi^+ \pi^-) = (5.9 \pm 1.1 \pm 0.5) \times 10^{-2}$ and $\mathcal{B}(B^- \rightarrow D^0 K^- \pi^+ \pi^-)/\mathcal{B}(B^- \rightarrow D^0 \pi^- \pi^+ \pi^-) = (9.4 \pm 1.3 \pm 0.9) \times 10^{-2}$, where the uncertainties are statistical and systematic, respectively. The $B^- \rightarrow D^0 K^- \pi^+ \pi^-$ decay is particularly interesting, as it can be used in a similar way to $B^- \rightarrow D^0 K^-$ to measure the CKM phase γ .

To be submitted to Physical Review Letters.

¹Authors are listed on the following pages.

The LHCb Collaboration

R. Aaij²³, C. Abellan Beteta^{35,n}, B. Adeva³⁶, M. Adinolfi⁴², C. Adrover⁶, A. Affolder⁴⁸,
Z. Ajaltouni⁵, J. Albrecht³⁷, F. Alessio³⁷, M. Alexander⁴⁷, G. Alkhazov²⁹,
P. Alvarez Cartelle³⁶, A.A. Alves Jr²², S. Amato², Y. Amhis³⁸, J. Anderson³⁹, R.B. Appleby⁵⁰,
O. Aquines Gutierrez¹⁰, F. Archilli^{18,37}, L. Arrabito⁵³, A. Artamonov³⁴, M. Artuso^{52,37},
E. Aslanides⁶, G. Auriemma^{22,m}, S. Bachmann¹¹, J.J. Back⁴⁴, D.S. Bailey⁵⁰, V. Balagura^{30,37},
W. Baldini¹⁶, R.J. Barlow⁵⁰, C. Barschel³⁷, S. Barsuk⁷, W. Barter⁴³, A. Bates⁴⁷, C. Bauer¹⁰,
Th. Bauer²³, A. Bay³⁸, I. Bediaga¹, S. Belogurov³⁰, K. Belous³⁴, I. Belyaev^{30,37},
E. Ben-Haim⁸, M. Benayoun⁸, G. Bencivenni¹⁸, S. Benson⁴⁶, J. Benton⁴², R. Bernet³⁹,
M.-O. Bettler¹⁷, M. van Beuzekom²³, A. Bien¹¹, S. Bifani¹², T. Bird⁵⁰, A. Bizzeti^{17,h},
P.M. Bjørnstad⁵⁰, T. Blake³⁷, F. Blanc³⁸, C. Blanks⁴⁹, J. Blouw¹¹, S. Blusk⁵², A. Bobrov³³,
V. Bocci²², A. Bondar³³, N. Bondar²⁹, W. Bonivento¹⁵, S. Borghi^{47,50}, A. Borgia⁵²,
T.J.V. Bowcock⁴⁸, C. Bozzi¹⁶, T. Brambach⁹, J. van den Brand²⁴, J. Bressieux³⁸, D. Brett⁵⁰,
M. Britsch¹⁰, T. Britton⁵², N.H. Brook⁴², H. Brown⁴⁸, A. Büchler-Germann³⁹, I. Burducea²⁸,
A. Bursche³⁹, J. Buytaert³⁷, S. Cadeddu¹⁵, O. Callot⁷, M. Calvi^{20,j}, M. Calvo Gomez^{35,n},
A. Camboni³⁵, P. Campana^{18,37}, A. Carbone¹⁴, G. Carboni^{21,k}, R. Cardinale^{19,i,37},
A. Cardini¹⁵, L. Carson⁴⁹, K. Carvalho Akiba², G. Casse⁴⁸, M. Cattaneo³⁷, Ch. Cauet⁹,
M. Charles⁵¹, Ph. Charpentier³⁷, N. Chiapolini³⁹, K. Ciba³⁷, X. Cid Vidal³⁶, G. Ciezarek⁴⁹,
P.E.L. Clarke^{46,37}, M. Clemencic³⁷, H.V. Cliff⁴³, J. Closier³⁷, C. Coca²⁸, V. Coco²³, J. Cogan⁶,
P. Collins³⁷, A. Comerma-Montells³⁵, F. Constantin²⁸, A. Contu⁵¹, A. Cook⁴², M. Coombes⁴²,
G. Corti³⁷, G.A. Cowan³⁸, R. Currie⁴⁶, C. D'Ambrosio³⁷, P. David⁸, P.N.Y. David²³,
I. De Bonis⁴, S. De Capua^{21,k}, M. De Cian³⁹, F. De Lorenzi¹², J.M. De Miranda¹,
L. De Paula², P. De Simone¹⁸, D. Decamp⁴, M. Deckenhoff⁹, H. Degaudenzi^{38,37},
L. Del Buono⁸, C. Deplano¹⁵, D. Derkach^{14,37}, O. Deschamps⁵, F. Dettori²⁴, J. Dickens⁴³,
H. Dijkstra³⁷, P. Diniz Batista¹, F. Domingo Bonal^{35,n}, S. Donleavy⁴⁸, F. Dordel¹¹,
A. Dosil Suárez³⁶, D. Dossett⁴⁴, A. Dovbnya⁴⁰, F. Dupertuis³⁸, R. Dzhelyadin³⁴, A. Dziurda²⁵,
S. Easo⁴⁵, U. Egede⁴⁹, V. Egorychev³⁰, S. Eidelman³³, D. van Eijk²³, F. Eisele¹¹,
S. Eisenhardt⁴⁶, R. Ekelhof⁹, L. Eklund⁴⁷, Ch. Elsasser³⁹, D. Elsby⁵⁵, D. Esperante Pereira³⁶,
L. Estève⁴³, A. Falabella^{16,14,e}, E. Fanchini^{20,j}, C. Färber¹¹, G. Fardell⁴⁶, C. Farinelli²³,
S. Farry¹², V. Fave³⁸, V. Fernandez Albor³⁶, M. Ferro-Luzzi³⁷, S. Filippov³², C. Fitzpatrick⁴⁶,
M. Fontana¹⁰, F. Fontanelli^{19,i}, R. Forty³⁷, M. Frank³⁷, C. Frei³⁷, M. Frosini^{17,f,37}, S. Furcas²⁰,
A. Gallas Torreira³⁶, D. Galli^{14,c}, M. Gandelman², P. Gandini⁵¹, Y. Gao³, J.-C. Garnier³⁷,
J. Garofoli⁵², J. Garra Tico⁴³, L. Garrido³⁵, D. Gascon³⁵, C. Gaspar³⁷, N. Gauvin³⁸,
M. Gersabeck³⁷, T. Gershon^{44,37}, Ph. Ghez⁴, V. Gibson⁴³, V.V. Gligorov³⁷, C. Göbel⁵⁴,
D. Golubkov³⁰, A. Golutvin^{49,30,37}, A. Gomes², H. Gordon⁵¹, M. Grabalosa Gándara³⁵,
R. Graciani Diaz³⁵, L.A. Granado Cardoso³⁷, E. Graugés³⁵, G. Graziani¹⁷, A. Grecu²⁸,
E. Greening⁵¹, S. Gregson⁴³, B. Gui⁵², E. Gushchin³², Yu. Guz³⁴, T. Gys³⁷, G. Haefeli³⁸,
C. Haen³⁷, S.C. Haines⁴³, T. Hampson⁴², S. Hansmann-Menzemer¹¹, R. Harji⁴⁹, N. Harnew⁵¹,
J. Harrison⁵⁰, P.F. Harrison⁴⁴, T. Hartmann⁵⁶, J. He⁷, V. Heijne²³, K. Hennessy⁴⁸,
P. Henrard⁵, J.A. Hernando Morata³⁶, E. van Herwijnen³⁷, E. Hicks⁴⁸, K. Holubyev¹¹,
P. Hopchev⁴, W. Hulsbergen²³, P. Hunt⁵¹, T. Huse⁴⁸, R.S. Huston¹², D. Hutchcroft⁴⁸,
D. Hynds⁴⁷, V. Iakovenko⁴¹, P. Ilten¹², J. Imong⁴², R. Jacobsson³⁷, A. Jaeger¹¹,
M. Jahjah Hussein⁵, E. Jans²³, F. Jansen²³, P. Jatton³⁸, B. Jean-Marie⁷, F. Jing³, M. John⁵¹,
D. Johnson⁵¹, C.R. Jones⁴³, B. Jost³⁷, M. Kaballo⁹, S. Kandybei⁴⁰, M. Karacson³⁷,
T.M. Karbach⁹, J. Keaveney¹², I.R. Kenyon⁵⁵, U. Kerzel³⁷, T. Ketel²⁴, A. Keune³⁸,

B. Khanji⁶, Y.M. Kim⁴⁶, M. Knecht³⁸, R. Koopman²⁴, P. Koppenburg²³, A. Kozlinskiy²³,
 L. Kravchuk³², K. Kreplin¹¹, M. Kreps⁴⁴, G. Krocker¹¹, P. Krokovny¹¹, F. Kruse⁹,
 K. Kruzelecki³⁷, M. Kucharczyk^{20,25,37,j}, T. Kvaratskheliya^{30,37}, V.N. La Thi³⁸, D. Lacarrere³⁷,
 G. Lafferty⁵⁰, A. Lai¹⁵, D. Lambert⁴⁶, R.W. Lambert²⁴, E. Lanciotti³⁷, G. Lanfranchi¹⁸,
 C. Langenbruch¹¹, T. Latham⁴⁴, C. Lazzeroni⁵⁵, R. Le Gac⁶, J. van Leerdam²³, J.-P. Lees⁴,
 R. Lefèvre⁵, A. Leflat^{31,37}, J. Lefrançois⁷, O. Leroy⁶, T. Lesiak²⁵, L. Li³, L. Li Gioi⁵,
 M. Lieng⁹, M. Liles⁴⁸, R. Lindner³⁷, C. Linn¹¹, B. Liu³, G. Liu³⁷, J. von Loeben²⁰,
 J.H. Lopes², E. Lopez Asamar³⁵, N. Lopez-March³⁸, H. Lu^{38,3}, J. Luisier³⁸, A. Mac Raighne⁴⁷,
 F. Machefert⁷, I.V. Machikhiliyan^{4,30}, F. Maciuc¹⁰, O. Maev^{29,37}, J. Magnin¹, S. Malde⁵¹,
 R.M.D. Mamunur³⁷, G. Manca^{15,d}, G. Mancinelli⁶, N. Mangiafave⁴³, U. Marconi¹⁴,
 R. Märki³⁸, J. Marks¹¹, G. Martellotti²², A. Martens⁸, L. Martin⁵¹, A. Martín Sánchez⁷,
 D. Martinez Santos³⁷, A. Massafferri¹, Z. Mathe¹², C. Matteuzzi²⁰, M. Matveev²⁹,
 E. Maurice⁶, B. Maynard⁵², A. Mazurov^{16,32,37}, G. McGregor⁵⁰, R. McNulty¹², M. Meissner¹¹,
 M. Merk²³, J. Merkel⁹, R. Messi^{21,k}, S. Miglioranzi³⁷, D.A. Milanese^{13,37}, M.-N. Minard⁴,
 J. Molina Rodriguez⁵⁴, S. Monteil⁵, D. Moran¹², P. Morawski²⁵, R. Mountain⁵², I. Mous²³,
 F. Muheim⁴⁶, K. Müller³⁹, R. Muresan^{28,38}, B. Muryn²⁶, B. Muster³⁸, M. Musy³⁵,
 J. Mylroie-Smith⁴⁸, P. Naik⁴², T. Nakada³⁸, R. Nandakumar⁴⁵, I. Nasteva¹, M. Nedos⁹,
 M. Needham⁴⁶, N. Neufeld³⁷, C. Nguyen-Mau^{38,o}, M. Nicol⁷, V. Niess⁵, N. Nikitin³¹,
 A. Nomerotski⁵¹, A. Novoselov³⁴, A. Oblakowska-Mucha²⁶, V. Obraztsov³⁴, S. Oggero²³,
 S. Ogilvy⁴⁷, O. Okhrimenko⁴¹, R. Oldeman^{15,d}, M. Orlandea²⁸, J.M. Otalora Goicochea²,
 P. Owen⁴⁹, K. Pal⁵², J. Palacios³⁹, A. Palano^{13,b}, M. Palutan¹⁸, J. Panman³⁷, A. Papanestis⁴⁵,
 M. Pappagallo⁴⁷, C. Parkes^{50,37}, C.J. Parkinson⁴⁹, G. Passaleva¹⁷, G.D. Patel⁴⁸, M. Patel⁴⁹,
 S.K. Paterson⁴⁹, G.N. Patrick⁴⁵, C. Patrignani^{19,i}, C. Pavel-Nicorescu²⁸, A. Pazos Alvarez³⁶,
 A. Pellegrino²³, G. Penso^{22,l}, M. Pepe Altarelli³⁷, S. Perazzini^{14,c}, D.L. Perego^{20,j},
 E. Perez Trigo³⁶, A. Pérez-Calero Yzquierdo³⁵, P. Perret⁵, M. Perrin-Terrin⁶, G. Pessina²⁰,
 A. Petrella^{16,37}, A. Petrolini^{19,i}, A. Phan⁵², E. Picatoste Olloqui³⁵, B. Pie Valls³⁵,
 B. Pietrzyk⁴, T. Pilar⁴⁴, D. Pinci²², R. Plackett⁴⁷, S. Playfer⁴⁶, M. Plo Casasus³⁶, G. Polok²⁵,
 A. Poluektov^{44,33}, E. Polcarpo², D. Popov¹⁰, B. Popovici²⁸, C. Potterat³⁵, A. Powell⁵¹,
 J. Prisciandaro³⁸, V. Pugatch⁴¹, A. Puig Navarro³⁵, W. Qian⁵², J.H. Rademacker⁴²,
 B. Rakotomiamanana³⁸, M.S. Rangel², I. Raniuk⁴⁰, G. Raven²⁴, S. Redford⁵¹, M.M. Reid⁴⁴,
 A.C. dos Reis¹, S. Ricciardi⁴⁵, K. Rinnert⁴⁸, D.A. Roa Romero⁵, P. Robbe⁷, E. Rodrigues^{47,50},
 F. Rodrigues², P. Rodriguez Perez³⁶, G.J. Rogers⁴³, S. Roiser³⁷, V. Romanovsky³⁴,
 M. Rosello^{35,n}, J. Rouvinet³⁸, T. Ruf³⁷, H. Ruiz³⁵, G. Sabatino^{21,k}, J.J. Saborido Silva³⁶,
 N. Sagidova²⁹, P. Sail⁴⁷, B. Saitta^{15,d}, C. Salzmann³⁹, M. Sannino^{19,i}, R. Santacesaria²²,
 C. Santamarina Rios³⁶, R. Santinelli³⁷, E. Santovetti^{21,k}, M. Sapunov⁶, A. Sarti^{18,l},
 C. Satriano^{22,m}, A. Satta²¹, M. Savrie^{16,e}, D. Savrina³⁰, P. Schaack⁴⁹, M. Schiller²⁴,
 S. Schleich⁹, M. Schlupp⁹, M. Schmelling¹⁰, B. Schmidt³⁷, O. Schneider³⁸, A. Schopper³⁷,
 M.-H. Schune⁷, R. Schwemmer³⁷, B. Sciascia¹⁸, A. Sciubba^{18,l}, M. Seco³⁶, A. Semennikov³⁰,
 K. Senderowska²⁶, I. Sepp⁴⁹, N. Serra³⁹, J. Serrano⁶, P. Seyfert¹¹, M. Shapkin³⁴,
 I. Shapoval^{40,37}, P. Shatalov³⁰, Y. Shcheglov²⁹, T. Shears⁴⁸, L. Shekhtman³³, O. Shevchenko⁴⁰,
 V. Shevchenko³⁰, A. Shires⁴⁹, R. Silva Coutinho⁴⁴, T. Skwarnicki⁵², A.C. Smith³⁷,
 N.A. Smith⁴⁸, E. Smith^{51,45}, K. Sobczak⁵, F.J.P. Soler⁴⁷, A. Solomin⁴², F. Soomro¹⁸,
 B. Souza De Paula², B. Spaan⁹, A. Sparkes⁴⁶, P. Spradlin⁴⁷, F. Stagni³⁷, S. Stahl¹¹,
 O. Steinkamp³⁹, S. Stoica²⁸, S. Stone^{52,37}, B. Storaci²³, M. Straticiuc²⁸, U. Straumann³⁹,
 V.K. Subbiah³⁷, S. Swientek⁹, M. Szczekowski²⁷, P. Szczypka³⁸, T. Szumlak²⁶, S. T'Jampens⁴,
 E. Teodorescu²⁸, F. Teubert³⁷, C. Thomas⁵¹, E. Thomas³⁷, J. van Tilburg¹¹, V. Tisserand⁴,

M. Tobin³⁹, S. Topp-Joergensen⁵¹, N. Torr⁵¹, E. Tournefier^{4,49}, M.T. Tran³⁸,
A. Tsaregorodtsev⁶, N. Tuning²³, M. Ubeda Garcia³⁷, A. Ukleja²⁷, P. Urquijo⁵², U. Uwer¹¹,
V. Vagnoni¹⁴, G. Valenti¹⁴, R. Vazquez Gomez³⁵, P. Vazquez Regueiro³⁶, S. Vecchi¹⁶,
J.J. Velthuis⁴², M. Veltri^{17,g}, B. Viaud⁷, I. Videau⁷, X. Vilasis-Cardona^{35,n}, J. Visniakov³⁶,
A. Vollhardt³⁹, D. Volyanskyy¹⁰, D. Voong⁴², A. Vorobyev²⁹, H. Voss¹⁰, S. Wandernoth¹¹,
J. Wang⁵², D.R. Ward⁴³, N.K. Watson⁵⁵, A.D. Webber⁵⁰, D. Websdale⁴⁹, M. Whitehead⁴⁴,
D. Wiedner¹¹, L. Wiggers²³, G. Wilkinson⁵¹, M.P. Williams^{44,45}, M. Williams⁴⁹, F.F. Wilson⁴⁵,
J. Wishahi⁹, M. Witek²⁵, W. Witzeling³⁷, S.A. Wotton⁴³, K. Wyllie³⁷, Y. Xie⁴⁶, F. Xing⁵¹,
Z. Xing⁵², Z. Yang³, R. Young⁴⁶, O. Yushchenko³⁴, M. Zavertyaev^{10,a}, F. Zhang³, L. Zhang⁵²,
W.C. Zhang¹², Y. Zhang³, A. Zhelezov¹¹, L. Zhong³, E. Zverev³¹, A. Zvyagin³⁷.

¹ *Centro Brasileiro de Pesquisas Físicas (CBPF), Rio de Janeiro, Brazil*

² *Universidade Federal do Rio de Janeiro (UFRJ), Rio de Janeiro, Brazil*

³ *Center for High Energy Physics, Tsinghua University, Beijing, China*

⁴ *LAPP, Université de Savoie, CNRS/IN2P3, Annecy-Le-Vieux, France*

⁵ *Clermont Université, Université Blaise Pascal, CNRS/IN2P3, LPC, Clermont-Ferrand, France*

⁶ *CPPM, Aix-Marseille Université, CNRS/IN2P3, Marseille, France*

⁷ *LAL, Université Paris-Sud, CNRS/IN2P3, Orsay, France*

⁸ *LPNHE, Université Pierre et Marie Curie, Université Paris Diderot, CNRS/IN2P3, Paris, France*

⁹ *Fakultät Physik, Technische Universität Dortmund, Dortmund, Germany*

¹⁰ *Max-Planck-Institut für Kernphysik (MPIK), Heidelberg, Germany*

¹¹ *Physikalisches Institut, Ruprecht-Karls-Universität Heidelberg, Heidelberg, Germany*

¹² *School of Physics, University College Dublin, Dublin, Ireland*

¹³ *Sezione INFN di Bari, Bari, Italy*

¹⁴ *Sezione INFN di Bologna, Bologna, Italy*

¹⁵ *Sezione INFN di Cagliari, Cagliari, Italy*

¹⁶ *Sezione INFN di Ferrara, Ferrara, Italy*

¹⁷ *Sezione INFN di Firenze, Firenze, Italy*

¹⁸ *Laboratori Nazionali dell'INFN di Frascati, Frascati, Italy*

¹⁹ *Sezione INFN di Genova, Genova, Italy*

²⁰ *Sezione INFN di Milano Bicocca, Milano, Italy*

²¹ *Sezione INFN di Roma Tor Vergata, Roma, Italy*

²² *Sezione INFN di Roma La Sapienza, Roma, Italy*

²³ *Nikhef National Institute for Subatomic Physics, Amsterdam, The Netherlands*

²⁴ *Nikhef National Institute for Subatomic Physics and Vrije Universiteit, Amsterdam, The Netherlands*

²⁵ *Henryk Niewodniczanski Institute of Nuclear Physics Polish Academy of Sciences, Kraków, Poland*

²⁶ *AGH University of Science and Technology, Kraków, Poland*

²⁷ *Soltan Institute for Nuclear Studies, Warsaw, Poland*

²⁸ *Horia Hulubei National Institute of Physics and Nuclear Engineering, Bucharest-Magurele, Romania*

²⁹ *Petersburg Nuclear Physics Institute (PNPI), Gatchina, Russia*

³⁰ *Institute of Theoretical and Experimental Physics (ITEP), Moscow, Russia*

³¹ *Institute of Nuclear Physics, Moscow State University (SINP MSU), Moscow, Russia*

³² *Institute for Nuclear Research of the Russian Academy of Sciences (INR RAN), Moscow, Russia*

³³ *Budker Institute of Nuclear Physics (SB RAS) and Novosibirsk State University, Novosibirsk, Russia*

³⁴ *Institute for High Energy Physics (IHEP), Protvino, Russia*

³⁵ *Universitat de Barcelona, Barcelona, Spain*

³⁶ *Universidad de Santiago de Compostela, Santiago de Compostela, Spain*

³⁷ *European Organization for Nuclear Research (CERN), Geneva, Switzerland*

³⁸ *Ecole Polytechnique Fédérale de Lausanne (EPFL), Lausanne, Switzerland*

³⁹ *Physik-Institut, Universität Zürich, Zürich, Switzerland*

⁴⁰ *NSC Kharkiv Institute of Physics and Technology (NSC KIPT), Kharkiv, Ukraine*

- ⁴¹*Institute for Nuclear Research of the National Academy of Sciences (KINR), Kyiv, Ukraine*
⁴²*H.H. Wills Physics Laboratory, University of Bristol, Bristol, United Kingdom*
⁴³*Cavendish Laboratory, University of Cambridge, Cambridge, United Kingdom*
⁴⁴*Department of Physics, University of Warwick, Coventry, United Kingdom*
⁴⁵*STFC Rutherford Appleton Laboratory, Didcot, United Kingdom*
⁴⁶*School of Physics and Astronomy, University of Edinburgh, Edinburgh, United Kingdom*
⁴⁷*School of Physics and Astronomy, University of Glasgow, Glasgow, United Kingdom*
⁴⁸*Oliver Lodge Laboratory, University of Liverpool, Liverpool, United Kingdom*
⁴⁹*Imperial College London, London, United Kingdom*
⁵⁰*School of Physics and Astronomy, University of Manchester, Manchester, United Kingdom*
⁵¹*Department of Physics, University of Oxford, Oxford, United Kingdom*
⁵²*Syracuse University, Syracuse, NY, United States*
⁵³*CC-IN2P3, CNRS/IN2P3, Lyon-Villeurbanne, France, associated member*
⁵⁴*Pontificia Universidade Católica do Rio de Janeiro (PUC-Rio), Rio de Janeiro, Brazil, associated to ²*
⁵⁵*University of Birmingham, Birmingham, United Kingdom*
⁵⁶*Physikalisches Institut, Universität Rostock, Rostock, Germany, associated to ¹¹*

- ^a*P.N. Lebedev Physical Institute, Russian Academy of Science (LPI RAS), Moscow, Russia*
^b*Università di Bari, Bari, Italy*
^c*Università di Bologna, Bologna, Italy*
^d*Università di Cagliari, Cagliari, Italy*
^e*Università di Ferrara, Ferrara, Italy*
^f*Università di Firenze, Firenze, Italy*
^g*Università di Urbino, Urbino, Italy*
^h*Università di Modena e Reggio Emilia, Modena, Italy*
ⁱ*Università di Genova, Genova, Italy*
^j*Università di Milano Bicocca, Milano, Italy*
^k*Università di Roma Tor Vergata, Roma, Italy*
^l*Università di Roma La Sapienza, Roma, Italy*
^m*Università della Basilicata, Potenza, Italy*
ⁿ*LIFAEELS, La Salle, Universitat Ramon Llull, Barcelona, Spain*
^o*Hanoi University of Science, Hanoi, Viet Nam*

The standard model (SM) of particle physics provides a good description of nature up to the TeV scale, yet many issues remain unresolved [1], including, but not limited to, the hierarchy problem, the preponderance of matter over antimatter in the Universe, and the need to explain dark matter. One of the main objectives of the LHC is to search for new physics beyond the Standard Model (SM) either through direct detection or through interference effects in b - and c -hadron decays. In the SM, the Cabibbo-Kobayashi-Maskawa (CKM) matrix [2] governs the strengths of weak charged-current interactions and their corresponding phases. Precise measurements on the CKM matrix parameters may reveal deviations from the consistency that is expected in the SM, making study of these decays a unique laboratory in which to search for physics beyond the standard model.

The most poorly constrained of the CKM parameters is the weak phase $\gamma \equiv \arg\left(-\frac{V_{ub}^*V_{ud}}{V_{cb}^*V_{cd}}\right)$. Its direct measurement reaches a precision of $10^\circ - 12^\circ$ [3, 4]. Two promising methods of measuring this phase are through the time-independent and time-dependent analyses of $B^- \rightarrow D^0 K^-$ [5, 6, 7] and $B_s^0 \rightarrow D_s^\mp K^\pm$ [8, 9], respectively. Both approaches can be extended to higher multiplicity modes, such as $\bar{B}^0 \rightarrow D^0 \bar{K}^{*0}$, $B^- \rightarrow D^0 K^- \pi^+ \pi^-$ [10] and $B_s^0 \rightarrow D_s^\mp K^\pm \pi^+ \pi^-$, which could provide a comparable level of sensitivity. The last two decays have not previously been observed.

In this Letter, we report first observations of the Cabibbo-suppressed (CS) $\bar{B}^0 \rightarrow D^+ K^- \pi^+ \pi^-$ and $B^- \rightarrow D^0 K^- \pi^+ \pi^-$ decays, where $D^+ \rightarrow K^- \pi^+ \pi^+$ and $D^0 \rightarrow K^- \pi^+$, where charge conjugation is implied throughout this Letter. These signal decays are normalized with respect to the topologically similar Cabibbo-favored (CF) $\bar{B}^0 \rightarrow D^+ \pi^- \pi^+ \pi^-$ and $B^- \rightarrow D^0 \pi^- \pi^+ \pi^-$ decays, respectively. For brevity, we use the notation X_d to refer to the recoiling $\pi^- \pi^+ \pi^-$ system in the CF decays and X_s for the $K^- \pi^+ \pi^-$ system in the CS decays.

The analysis presented here is based on 35 pb^{-1} of data collected with the LHCb detector in 2010. For these measurements, the most important parts of LHCb are the vertex detector (VELO), the charged particle tracking system, the ring imaging Cherenkov detectors (RICH) and the trigger. The VELO is instrumental in separating particles coming from heavy quark decays and those emerging directly from pp interactions, by providing an impact parameter (IP) resolution of about $16 \mu\text{m} + 30 \mu\text{m}/p_T$ (transverse momentum, p_T in GeV/c). The tracking system measures charged particles' momenta with a resolution of $\sigma_p/p \sim 0.4\%(0.6\%)$ at 5 (100) GeV/c . The RICH detectors are important to identify kaons and suppress the large backgrounds from pions misidentified as kaons. Events are selected by a two-level trigger system. The first level is hardware-based, and requires either a large transverse energy deposition in the calorimeter system, or a high p_T muon or pair of muons detected in the muon system. The second level, the high-level trigger, uses simplified versions of the offline software to reconstruct decays of b - and c -hadrons both inclusively and exclusively. Candidates passing the trigger selections are saved and used for offline analysis. A more detailed description of the LHCb detector can be found elsewhere [11]. In this analysis the signal and normalization modes are topologically identical, allowing loose trigger requirements to be made with small associated uncertainty.

In particular, we exploit the fact that b -hadrons are produced in pairs in pp collisions, and include events that were triggered by the decay products of either the signal b -hadron or the other b -hadron in the event. This requirement increases the efficiency of our trigger selection by about 80% compared to the trigger selections requiring the signal b -hadron to be responsible for triggering the event, as was done in Ref. [12].

The selection criteria used to reconstruct the $\bar{B}^0 \rightarrow D^+\pi^-\pi^+\pi^-$ and $B^- \rightarrow D^0\pi^-\pi^+\pi^-$ final states are described in Ref. [12]. The Cabibbo suppression results in about a factor of 20 lower rate. To improve the signal-to-background ratio in the CS decay modes, additional selection requirements are imposed, and they are applied to both the signal and normalization modes. The B meson candidate is required to have $p_T > 4$ GeV/ c , $IP < 60$ μm with respect to its associated primary vertex (PV), where the associated PV is the one having the smallest impact parameter χ^2 with respect to the track. We also require the flight distance $\chi^2 > 144$, where the χ^2 is with respect to the zero flight distance hypothesis, and the vertex $\chi^2/\text{ndf} < 5$, where ndf represents the number of degrees of freedom in the fit. The last requirement is also applied to the vertices associated with X_d and X_s . Three additional criteria are applied only to the CS modes. First, to remove the peaking backgrounds from $B \rightarrow DD_s^-$, $D_s^- \rightarrow K^-\pi^+\pi^-$, we veto events where the invariant mass, $M(X_s)$, is within 20 MeV/ c^2 of the D_s mass. Information from the RICH is critical to reduce background from the CF decay modes. This suppression is accomplished by requiring the kaon in X_s to have $p < 100$ GeV/ c (above which there is minimal K/π separation from the RICH), and the difference in log-likelihoods between the kaon and pion hypotheses to satisfy $\Delta\ln\mathcal{L}(K - \pi) > 8$. The latter requirement is determined by optimizing $N_S/\sqrt{N_S + N_B}$, where we assume 100 signal events ($\sim 1/20$ of the CF decay yields) prior to any particle identification (PID) selection requirement, and the combinatorial background yield, N_B , is taken from the high B -mass sideband (5350-5580 MeV/ c^2). We also make a loose PID requirement of $\Delta\ln\mathcal{L}(K - \pi) < 10$ on the pions in X_s and X_d .

Selection and trigger efficiencies are determined from simulation. Events are produced using PYTHIA [13] and long-lived particles are decayed using EVTGEN [14]. The detector response is simulated with GEANT4 [15]. The $DK^-\pi^+\pi^-$ final states are assumed to include 50% $DK_1(1270)^-$ and 20% $DK_1(1400)^-$, with smaller contributions from $DK_2(1430)^-$, $DK^*(1680)^-$, $D\bar{K}^*(892)^0\pi^-$ and $D_1(2420)K^-$. The resonances included in the simulation of the X_d system are described in Ref. [12]. The relative efficiencies, including selection and trigger, but not PID selection, are determined to be $\epsilon_{\bar{B}^0 \rightarrow D^+K^-\pi^+\pi^-} / \epsilon_{\bar{B}^0 \rightarrow D^+\pi^-\pi^+\pi^-} = 1.05 \pm 0.04$ and $\epsilon_{B^- \rightarrow D^0K^-\pi^+\pi^-} / \epsilon_{B^- \rightarrow D^0\pi^-\pi^+\pi^-} = 0.942 \pm 0.036$, where the uncertainties are statistical only. The efficiencies have a small dependence on the contributing resonances and their daughters' masses, and we therefore do not necessarily expect the ratios to be equal to unity. Moreover, the additional selections on the CS modes contribute to small differences between the signal and normalization modes' efficiencies.

The PID efficiencies are determined in bins of track momentum and pseudorapidity (η) using the D^0 daughters from $D^{*\pm} \rightarrow \pi_s^\pm D^0$, $D^0 \rightarrow K^-\pi^+$ calibration data, where the particles are identified without RICH information using the charge of the soft pion, π_s . The kinematics of the kaon in the X_s system are taken from simulation after all offline and

trigger selections. Applying the PID efficiencies to the simulated decays, we determine the efficiencies for the kaon to pass the $\Delta \ln \mathcal{L}(K - \pi) > 8$ requirement to be $(75.9 \pm 1.5)\%$ for $\bar{B}^0 \rightarrow D^+ K^- \pi^+ \pi^-$ and $(79.2 \pm 1.5)\%$ for $B^- \rightarrow D^0 K^- \pi^+ \pi^-$.

Invariant mass distributions for the normalization and signal modes are shown in Fig. 1. Signal yields are determined through unbinned maximum likelihood fits to the sum of signal and several background components. The signal distributions are parametrized as the sum of two Gaussian functions with common means, and shape parameters, σ_{core} and f_{core} that represent the width and area fraction of the narrower (core) Gaussian portion, and $r_w \equiv \sigma_{\text{wide}}/\sigma_{\text{core}}$, which is the ratio of the wider to narrower Gaussian width.

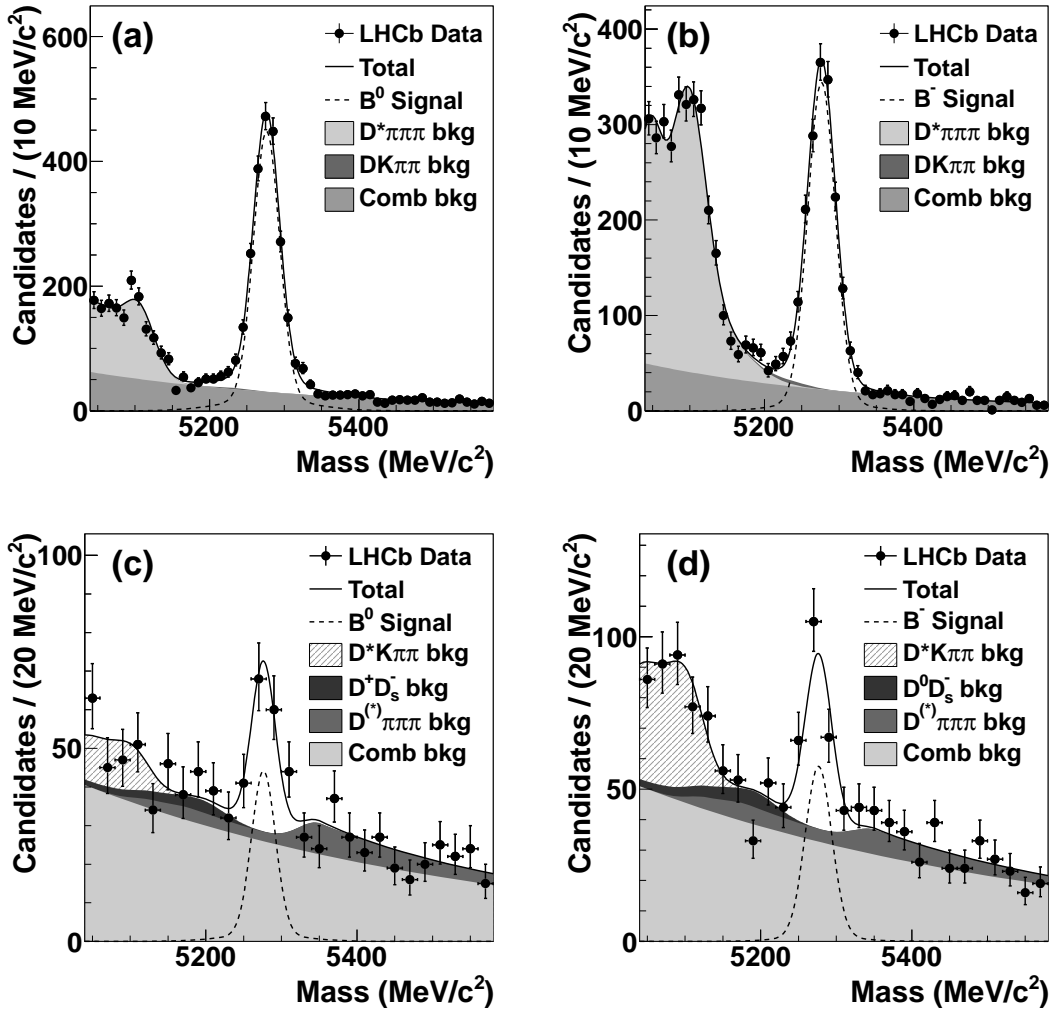


Figure 1: Invariant mass distributions for (a) $\bar{B}^0 \rightarrow D^+ \pi^- \pi^+ \pi^-$, (b) $B^- \rightarrow D^0 \pi^- \pi^+ \pi^-$, (c) $\bar{B}^0 \rightarrow D^+ K^- \pi^+ \pi^-$ and (d) $B^- \rightarrow D^0 K^- \pi^+ \pi^-$ candidates from 35 pb^{-1} of data for all selected candidates. Fits as described in the text are overlaid.

The CF modes are first fit with f_{core} and r_w constrained to the values from simulation

within their uncertainties, while σ_{core} is left as a free parameter since simulation underestimates the mass resolution by $\sim 10\%$. For the CF decay mode fits, the background shapes are the same as those described in Ref. [12]. The resulting signal shape parameters from the CF decay fits are then fixed in subsequent fits to the CS decay modes. For σ_{core} , the values from the CF decay fits are scaled by width correction factors (~ 0.95) obtained from MC simulations.

For the CS decays, invariant mass shapes of specific peaking backgrounds from other b -hadron decays are determined from MC simulation. The largest of these backgrounds comes from $D^{(*)}\pi^-\pi^+\pi^-$ decays, where one of the π^- passes the $\Delta\ln\mathcal{L}(K-\pi) > 8$ requirement and is misidentified as a K^- . To determine the fraction of events in which this occurs, we use measured PID fake rates (π faking K) obtained from $D^{*\pm}$ calibration data (binned in (p, η)), and apply them to each π^- in $D\pi^-\pi^+\pi^-$ simulated events. A decay is considered a fake if either pion has $p < 100$ GeV/ c , and a randomly generated number in the interval from $[0, 1]$ is less than that pion's determined fake rate. The pion's mass is then replaced by the kaon's mass, and the invariant mass of the b -hadron is recomputed. The resulting spectrum is then fitted using a Crystal Ball [16] lineshape and its parameters are fixed in fits to data. Using this method, we find the same cross-feed rate of $(4.4 \pm 0.7)\%$ for both $\bar{B}^0 \rightarrow D^+\pi^-\pi^+\pi^-$ and $B^- \rightarrow D^0\pi^-\pi^+\pi^-$ into $\bar{B}^0 \rightarrow D^+K^-\pi^+\pi^-$ and $B^- \rightarrow D^0K^-\pi^+\pi^-$, respectively, where the uncertainty includes both statistical and systematic sources. A similar procedure is used to obtain the $D^*\pi^-\pi^+\pi^-$ background yields and shapes. The background yields are obtained by multiplying the observed CF signal yields in data by the cross-feed rates and the fraction of background in the region of the mass fit (5040–5580 MeV/ c^2).

We also account for backgrounds from the decays $B \rightarrow DD_s^-$, $D_s^- \rightarrow K^-K^+\pi^-$, where the K^+ is misidentified as a π^+ . The yields of these decays are lower, but are offset by a larger fake rate since the PID requirement on the particles assumed to be pions is significantly looser ($\Delta\ln\mathcal{L}(K-\pi) < 10$). Using the same technique as described above, the fake rate is found to be $(24 \pm 2)\%$. The fake yield from this source is then computed from the product of the measured yield of $\bar{B}^0 \rightarrow D^+D_s^-$ in data ($161 \pm 14(\text{stat})$) and the above fake rate. The $B^- \rightarrow D^0D_s^-$ yield was not directly measured, but was determined from known branching fractions [17] and efficiencies from simulation. Additional uncertainty due to these extrapolations is included in the estimated $B^- \rightarrow D^0D_s^-$ background yield.

The last sources of background, which do not contribute to the signal regions, are from $D^*K^-\pi^+\pi^-$, where the soft pion or photon from the D^* is lost. The shapes of these low mass backgrounds are taken from the fitted $D^*\pi^-\pi^+\pi^-$ shapes in the $D\pi^-\pi^+\pi^-$ mass fits, and the yield ratios $N(D^*K^-\pi^+\pi^-)/N(DK^-\pi^+\pi^-)$, are constrained to be equal to the ratios obtained from CF mode fits with a 25% uncertainty.

The combinatorial background is assumed to have an exponential shape. A summary of the signal shape parameters and the specific b -hadron backgrounds used in the CS signal mode fits is given in Table 1.

The fitted yields are 2126 ± 69 $\bar{B}^0 \rightarrow D^+\pi^-\pi^+\pi^-$ and 1630 ± 57 and $B^- \rightarrow D^0\pi^-\pi^+\pi^-$ events. For the CS modes, we find 90 ± 16 $\bar{B}^0 \rightarrow D^+K^-\pi^+\pi^-$ and 130 ± 17 $B^- \rightarrow D^0K^-\pi^+\pi^-$ signal decays. The CS decay signals have significances of 7.2 and 9.0, respec-

tively, calculated as $\sqrt{-2\ln(\mathcal{L}_0/\mathcal{L}_{\max})}$, where \mathcal{L}_{\max} and \mathcal{L}_0 are the fit likelihoods with the signal yields left free and fixed to zero, respectively. In evaluating these significances, we remove the constraint on $N(D^*K^-\pi^+\pi^-)/N(DK^-\pi^+\pi^-)$, which would otherwise bias the $D^*K^-\pi^+\pi^-$ yield toward zero and inflate \mathcal{L}_0 . Varying the signal or background shapes or normalizations within their uncertainties has only a minor impact on the significances. We therefore observe for the first time the $\bar{B}^0 \rightarrow D^+K^-\pi^+\pi^-$ and $B^- \rightarrow D^0K^-\pi^+\pi^-$ decay modes.

Table 1: Summary of parameters used in the CS mass fits. Values without uncertainties are fixed in the CS mode fits, and values with uncertainties are included with a Gaussian constraint with central values and widths as indicated.

Parameter	$D^+K^-\pi^+\pi^-$	$D^0K^-\pi^+\pi^-$
Mean mass (MeV/ c^2)	5276.3	5276.5
σ_{core} (MeV/ c^2)	15.7	17.5
f_{core}	0.88	0.93
$\sigma_{\text{wide}}/\sigma_{\text{core}}$	3.32	2.82
$N(D\pi\pi\pi)$	63 ± 10	48 ± 8
$N(D^*\pi\pi\pi)$	47 ± 9	107 ± 18
$N(DD_s)$	23 ± 3	38 ± 8
$N(D^*K\pi\pi)/N(DK\pi\pi)$	0.62 ± 0.16	1.86 ± 0.46

The ratios of branching fractions are given by

$$\frac{\mathcal{B}(H_b \rightarrow H_c K^-\pi^+\pi^-)}{\mathcal{B}(H_b \rightarrow H_c \pi^-\pi^+\pi^-)} = \frac{Y^{\text{CS}}}{Y^{\text{CF}}} \times \epsilon_{\text{tot}}^{\text{rel}},$$

where Y^{CF} (Y^{CS}) are the fitted yields in the CF (CS) decay modes, and $\epsilon_{\text{tot}}^{\text{rel}}$ are the products of the relative selection and PID efficiencies discussed previously. The results for the branching fractions are

$$\frac{\mathcal{B}(\bar{B}^0 \rightarrow D^+K^-\pi^+\pi^-)}{\mathcal{B}(\bar{B}^0 \rightarrow D^+\pi^-\pi^+\pi^-)} = (5.9 \pm 1.1 \pm 0.5) \times 10^{-2},$$

$$\frac{\mathcal{B}(B^- \rightarrow D^0K^-\pi^+\pi^-)}{\mathcal{B}(B^- \rightarrow D^0\pi^-\pi^+\pi^-)} = (9.4 \pm 1.3 \pm 0.9) \times 10^{-2},$$

where the first uncertainties are statistical and the second are from the systematic sources discussed below.

Most systematic uncertainties cancel in the measured ratios of branching fractions; only those that do not are discussed below. One source of uncertainty comes from modeling of the $K^-\pi^+\pi^-$ final state. In Ref. [12], we compared the p and p_{T} spectra of π^\pm from

X_d , and they agreed well with simulation. We have an insufficiently large data sample to make such a comparison in the CS signal decay modes. The departure from unity of the efficiency ratios obtained from simulation are due to differences in the p_T spectra between the X_d daughters in CF decays and the X_s daughters in the CS decays. These differences depend on the contributing resonances and the daughters' masses. We take the full difference of the relative efficiencies from unity (4.6% for \bar{B}^0 and 6.1% for B^-) as a systematic uncertainty.

The kaon PID efficiency includes uncertainties from the limited size of the data set used for the efficiency determination, the limited number of events in the MC sample over which we average, and possible systematic effects described below. The statistical precision is taken as the RMS width of the kaon PID efficiency distribution obtained from pseudo-experiments, where in each one, the kaon PID efficiencies in each (p, η) bin are fluctuated about their nominal values within their uncertainties. This contributes 1.5% to the overall kaon PID efficiency uncertainty. We also consider the systematic error in using the D^* data sample to determine the PID efficiency. The procedure is tested by comparing the kaon PID efficiency using a MC-derived efficiency matrix with the efficiency obtained by directly requiring $\Delta \ln \mathcal{L}(K - \pi) > 8$ on the kaon from X_s in the signal MC. The relative difference is found to be $(3.6 \pm 1.9)\%$. We take the full difference of 3.6% as a potential systematic error. The total kaon PID uncertainty is 3.9%.

The fit model uncertainty includes 3% systematic uncertainty in the yields from the normalization modes [12]. The uncertainties in the CS signal fits are obtained by varying each of the signal shape parameters within the uncertainty obtained from the CF mode data fits. The signal shape parameter uncertainties are 2.7% for \bar{B}^0 and 2.5% for B^- . For the specific b -hadron background shapes, we obtain the uncertainty by refitting the data 100 times, where each fit is performed with all background shapes fluctuated within their covariances and subsequently fixed in the fit to data (1%). The uncertainties in the yields from the assumed exponential shape for the combinatorial background are estimated by taking the difference in yields between the nominal fit and one with a linear shape for the combinatorial background (2%). In total, the relative yields are uncertain by 4.5% for \bar{B}^0 and 4.4% for B^- .

The limited number of MC events for determining the relative efficiencies contributes 4.1% and 3.8% to the \bar{B}^0 and B^- branching fraction ratio uncertainties, respectively. Other sources of uncertainty are negligible. In total, the uncertainties on the ratio of branching fractions are 8.6% for \bar{B}^0 and 9.3% for B^- .

We have also looked at the substructures that contribute to the CS final states. Figure 2 shows the observed distributions of (a) $K^-\pi^+\pi^-$ invariant mass, (b) $M(D^0\pi^+\pi^-) - M(D^0)$ invariant mass difference, (c) $K^-\pi^+$ invariant mass, and (d) $\pi^+\pi^-$ invariant mass for $B^- \rightarrow D^0 K^-\pi^+\pi^-$. We show events in the B mass signal region, defined to have an invariant mass from 5226–5326 MeV/ c^2 , and events from the high-mass sideband (5350–5550 MeV/ c^2), scaled by the ratio of expected background yields in the signal region relative to the sideband region. An excess of events is observed predominantly in the low $K^-\pi^+\pi^-$ mass region near 1300–1400 MeV/ c^2 , and the number of signal events decreases with increasing mass. In Fig. 2(b) there appears to be an excess of

~ 10 events in the region around $550\text{--}600\text{ MeV}/c^2$, which suggests contributions from $D_1(2420)^0$ or $D_2^*(2460)^0$ meson decays. These decays can also be used for measuring the weak phase γ [18]. This yield, relative to the total, is similar to what was observed in $B^- \rightarrow D^0\pi^-\pi^+\pi^-$ decays [12]. Figures 2(c) and (d) show significant enhancements at the \bar{K}^{*0} and ρ^0 masses, consistent with decays of excited strange states, such as the $K_1(1270)^-$, $K_1(1400)^-$ and $K^*(1410)^-$. Similar distributions are observed for the $\bar{B}^0 \rightarrow D^+K^-\pi^+\pi^-$, except that no excess of events is observed near $550\text{--}600\text{ MeV}/c^2$ in the $M(D^0\pi^+\pi^-) - M(D^0)$ invariant mass difference.

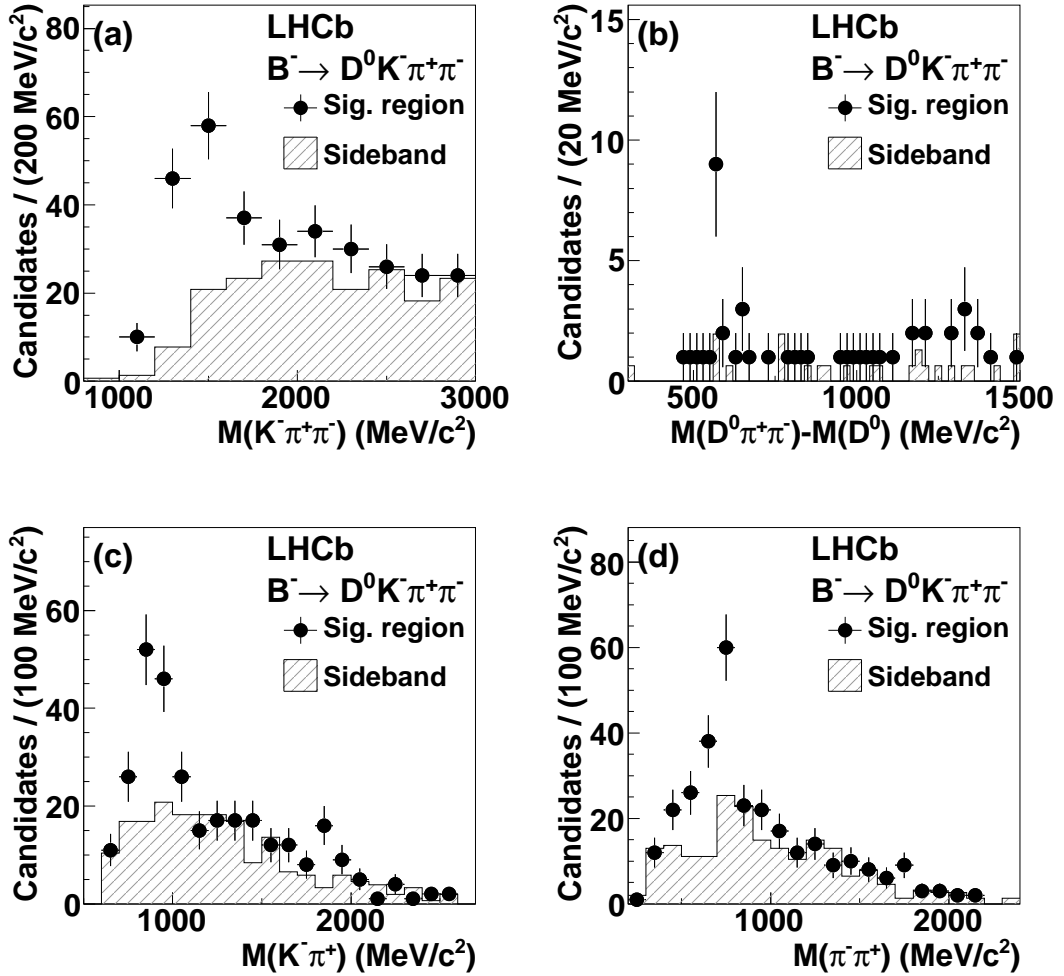


Figure 2: Invariant masses within the $B^- \rightarrow D^0 K^- \pi^+ \pi^-$ system. Shown are (a) $M(K^- \pi^+ \pi^-)$, (b) $M(D^0 \pi^+ \pi^-) - M(D^0)$, (c) $M(K^- \pi^+)$, and (d) $M(\pi^- \pi^+)$. The points with error bars correspond to the signal region, and the hatched histograms represent the scaled sideband region.

In summary, we report first observations of the Cabibbo-suppressed decay modes

$\bar{B}^0 \rightarrow D^+ K^- \pi^+ \pi^-$ and $B^- \rightarrow D^0 K^- \pi^+ \pi^-$ and measurements of their branching fractions relative to $\bar{B}^0 \rightarrow D^+ \pi^- \pi^+ \pi^-$ and $B^- \rightarrow D^0 \pi^- \pi^+ \pi^-$. The $B^- \rightarrow D^0 K^- \pi^+ \pi^-$ decay is particularly interesting because, with more data, it can be used to measure the weak phase γ , using similar techniques as for $B^- \rightarrow D^0 K^-$ and $\bar{B}^0 \rightarrow D^0 \bar{K}^{*0}$.

Acknowledgements

We express our gratitude to our colleagues in the CERN accelerator departments for the excellent performance of the LHC. We thank the technical and administrative staff at CERN and at the LHCb institutes, and acknowledge support from the National Agencies: CAPES, CNPq, FAPERJ and FINEP (Brazil); CERN; NSFC (China); CNRS/IN2P3 (France); BMBF, DFG, HGF and MPG (Germany); SFI (Ireland); INFN (Italy); FOM and NWO (The Netherlands); SCSR (Poland); ANCS (Romania); MinES of Russia and Rosatom (Russia); MICINN, XuntaGal and GENCAT (Spain); SNSF and SER (Switzerland); NAS Ukraine (Ukraine); STFC (United Kingdom); NSF (USA). We also acknowledge the support received from the ERC under FP7 and the Region Auvergne.

References

- [1] C. Quigg, *Ann. Rev. Nucl. Part. Sci.* **59** (2009) 505, [arXiv:0905.3187](#).
- [2] N. Cabibbo, *Phys. Rev. Lett.* **10** (1963) 531; M. Kobayashi and T. Maskawa, *Prog. Theor. Phys.* **49** (1973) 652.
- [3] A. Bevan *et al.*, *Nucl. Phys. Proc. Suppl.* **209** (2010) 109. Additional information available at www.utfit.org.
- [4] J. Charles *et al.*, *Phys. Rev.* **D84** (2011) 033005, [arXiv:1106.4041](#). Updated results and plots available at ckmfitter.in2p3.fr.
- [5] I. Dunietz, *Phys. Lett.* **B270** (1991) 75; I. Dunietz, *Z. Phys.* **C56** (1992) 129; D. Atwood, G. Eilam, M. Gronau, and A. Soni, *Phys. Lett.* **B341** (1995) 372, [arXiv:hep-ph/9409229](#); D. Atwood, I. Dunietz, and A. Soni, *Phys. Rev. Lett.* **78** (1997) 3257, [arXiv:hep-ph/9612433](#).
- [6] M. Gronau and D. London, *Phys. Lett.* **B253** (1991) 483; M. Gronau and D. Wyler, *Phys. Lett.* **B265** (1991) 172.
- [7] A. Giri, Y. Grossman, A. Soffer, and J. Zupan, *Phys. Rev.* **D68** (2003) 054018, [arXiv:hep-ph/0303187](#).
- [8] R. Aleksan, I. Dunietz, and B. Kayser, *Z. Phys.* **C54** (1992) 653.
- [9] I. Dunietz, *Phys. Rev.* **D52** (1995) 3048, [arXiv:hep-ph/9501287](#).

- [10] M. Gronau, Phys. Lett. **B557** (2003) 198, [arXiv:hep-ph/0211282](#).
- [11] LHCb Collaboration, Alves, A. Augusto Jr. and others, JINST **3** (2008) S08005.
- [12] LHCb Collaboration, R. Aaij *et al.*, Phys. Rev. **D84** (2011) 092001, [arXiv:1109.6831](#).
- [13] T. Sjöstrand, S. Mrenna, and P. Z. Skands, JHEP **05** (2006) 026, [arXiv:hep-ph/0603175](#).
- [14] D. J. Lange, Nucl. Instrum. Meth. **A462** (2001) 152.
- [15] GEANT4, S. Agostinelli *et al.*, Nucl. Instrum. Meth. **A506** (2003) 250.
- [16] T. Skwarnicki, *A study of the radiative cascade transitions between the Upsilon-prime and Upsilon resonances*. PhD thesis, Institute of Nuclear Physics, Krakow, Poland, 1986.
- [17] Particle Data Group, K. Nakamura *et al.*, J. Phys. **G37** (2010) 075021.
- [18] N. Sinha, Phys. Rev. **D70** (2004) 097501, [arXiv:hep-ph/0405061](#).